Automated Boulder Detection and Measuring in HiRISE images

Don R. Hood[1] (dhood7@lsu.edu) , S. Karunatillake[1], C.I. Fassett[2], S.F. Sholes[3]

1: Louisiana State University Geology and Geophysics, Planetary Science Lab, 2: NASA Marshall Space Flight Center
3: University of Washington Earth and Space Sciences & Astrobiology,

Abstract #2437

Introduction

Images taken by the High Resolution Imaging Science Experiment (HiRISE) show that meter-scale boulders, as observed by landers and rovers, are present across the entire surface of Mars [1], [2]. Quantifying estimates of these boulder populations, including their size and location, can inform Martian pedogenesis, surface weathering, impact processes, and mass wasting processes [3], [4]. However, manual measurement of boulder populations is time intensive, and cannot be applied at large scales (e.g. more than a few square km of surface area). To facilitate this, we have developed a Python-based algorithm to automatically identify, locate, and measure boulders on the martian surface. This set of tools and programs is collected in a python library called the Martian Boulder Automatic Recognition System: MBARS. This is designed as a publicly available (via online source e.g. GitHub) toolset to enable science and allow modification and improvement by the larger community.

Methodology

- Modeled after method in Golombek 2008 [1]
- Shadowed areas identified via intensity thresholding (Figure 2,4)
- Shadows outlined via watershed [6]
- Ellipses fit with Orthogonal Distance Regression (Figure 3,5)
- Boulder width and height interpreted from shadow geometry (Figure 3)

Performance and Verification

- On 16 GB, 4 Core 3.6 GHz processor, full image processes in ~10 hours
- Handles data errors smoothly
- Algorithm tested against existing datasets:
  - o Measurements by other algorithms [1], [2]
  - o Manual measurements (Figure 6,7)
  - o Objects of known size (landers, rovers, and measured rocks)
- 3 sections of PSP_007718_2350 are main test dataset
- Testing emphasizes accuracy with populations and individual objects
- Cumulative Fractional Area, Size-Frequency distributions: key population comparators

Application

- MBARS aids in scientific investigation of martian surface processes:
  - o Boulder clustering on periglacial terrain [4]
  - o Boulder erosion and weathering [3], [7]
  - o Impact ejecta studies [8]
- Landing site characterization and terrain recognition
- Planned application to lunar images

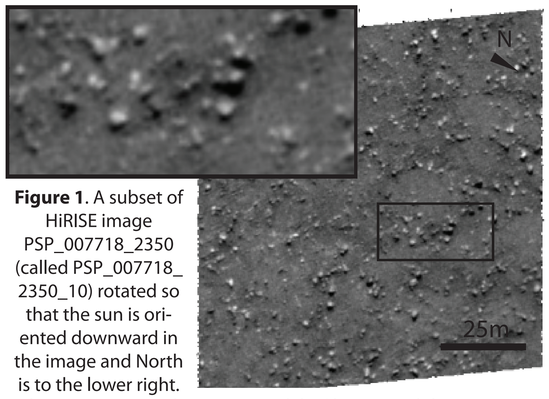

Figure 1. A subset of HiRISE image PSP_007718_2350 (called PSP_007718_2350_10) rotated so that the sun is oriented downward in the image and North is to the lower right. This image is in rocky area in Acidalia Planitia, with low topography and abundant rocks, an ideal test target for MBARS. The image inset is ~30m across and used in all following images.

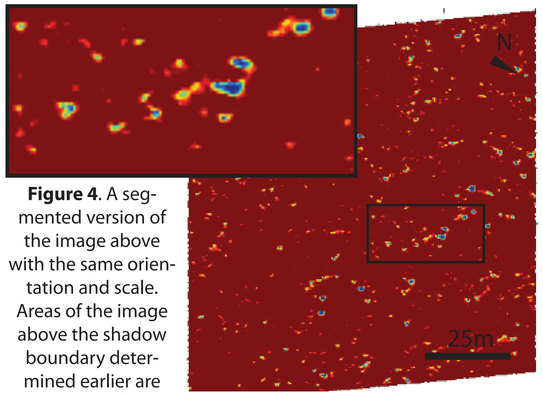

Figure 4. A segmented version of the image above with the same orientation and scale. Areas of the image above the shadow boundary determined earlier are mapped to a single value while the pixels below the value are unaltered. This image feeds into our watershed method-based shadow identification method. Seeds for watershed are determined by local minima in the shadows, which helps split merged shadows. This and the remaining images show results using a gamma value of 0.7 and boundary of 0.1

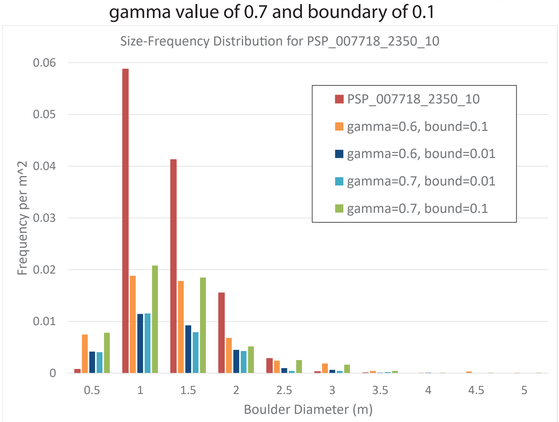

Figure 6. A size-frequency distribution for manual and automated results for PSP_007718_2350, showing the area-normalized frequency of boulders depending on their diameter. The manual data is shown in red, labeled as PSP_007718_2350_10, and automated results are named according to their running parameters gamma and bound. This clearly shows the tendency of MBARS to underestimate the abundance of small boulders and overestimate the abundance of larger boulders.

Algorithm Workflow

- **Partitioning**: Improves speed, user can control level of partitioning
- **Gamma Filter**: Stretches low-value pixels, precise sampling of penumbra, low gamma = intense stretch
- **Rotate Image**: Orienting image in sun direction simplifies ellipse fitting
- **Separate Shadows**: Shadows identified, merged shadows are split
- **Fit shadows**: Method shown in figure 3, results in Figure 5
- **Boulder measure**: Boulder widths and heights are measured, stored for later analysis (Figure 6,7)

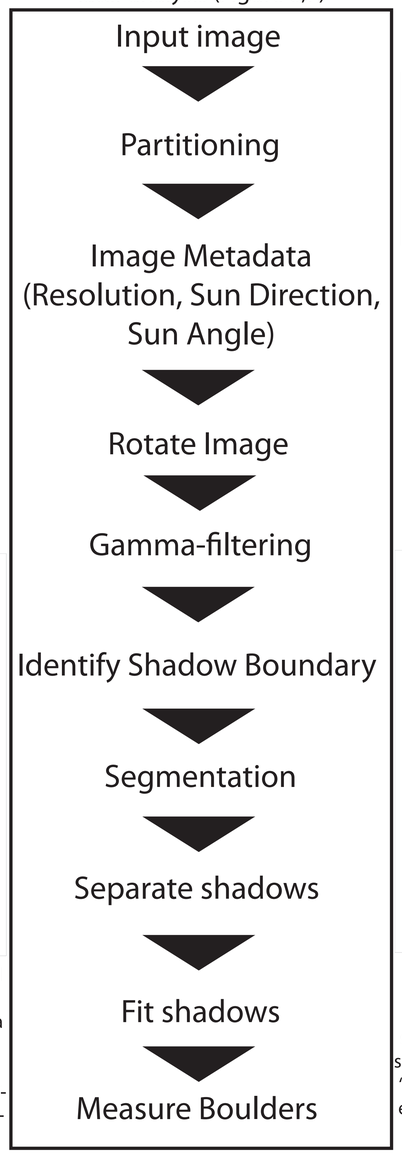

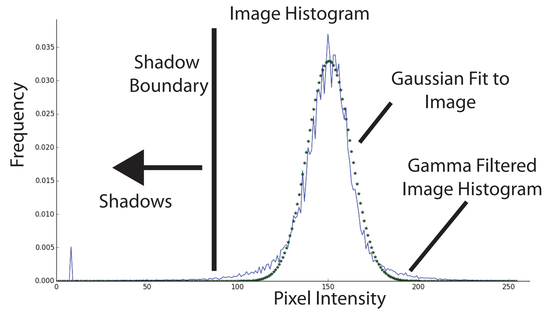

Figure 2. We determine the "shadow intensity" based on a gaussian fit to the image intensity histogram. We fit a gaussian (green stars) to the image histogram (blue line) and select a boundary based on the fit. The user sets a fraction (say .01) to select as the boundary, the program calculates the intensity where the fit frequency equals that fraction of its maximum value. Larger fractions include more pixels as 'shadowed', increasing estimated boulder size.

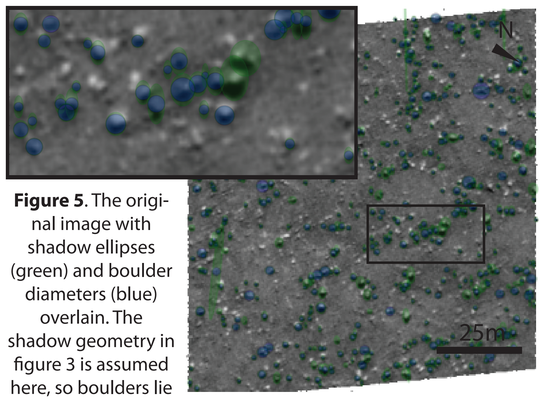

Figure 5. The original image with shadow ellipses (green) and boulder diameters (blue) overlain. The shadow geometry in figure 3 is assumed here, so boulders lie at the center of the shadow ellipse. The inset highlights the ability of the watershed method to split merged shadows, accurately separating the continuous shadowed area.

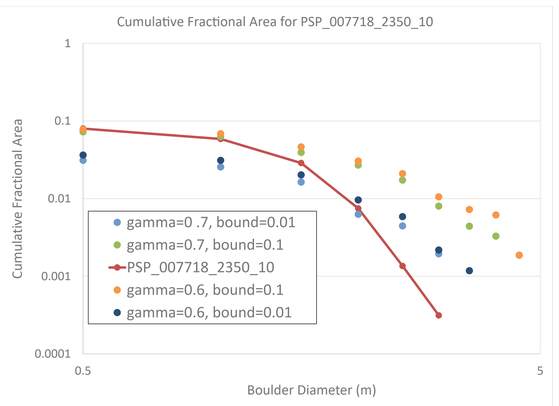

Figure 7. A cumulative fractional area plot for manual and automated results for PSP_007718_2350, showing the total fractional area of all boulders above a given diameter. The manual data is shown in red, labeled as PSP_007718_2350_10, and automated results are named according to their running parameters "gamma" and "bound". The effect of changing these running parameters is apparent here, with estimated boulder size increasing with higher bound and with decreasing with higher gamma.

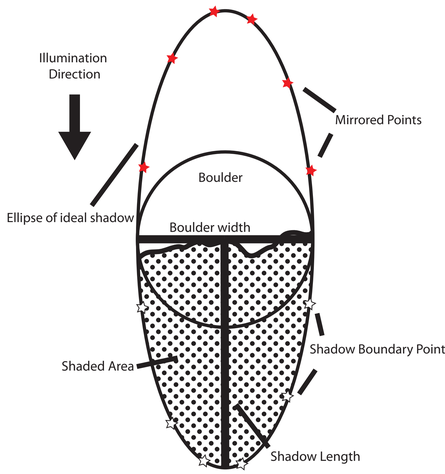

Figure 3. Our model geometry for individual boulders and fitting method. On flat ground with the sun coming from the north, a spheroidal boulder casts a half-elliptical shadow (umbra+penumbra) where the minor axis is equal to the boulder diameter and the semi-major axis determined by the boulder height. We mirror points along the shadow boundary (white stars) across the sunward end of the shadow to map the outline of the full ellipse (red stars).

Conclusions & Future Work

- MBARS tends to miss smaller boulders and overestimate boulder diameters
- False positives not observed in images
- Comparison with published algorithms promising
- Will fully explore parameter space to identify most accurate settings
- Cut processing time down to <1 hour
  - o Parallelization is key step

Acknowledgements & References

This work is supported by the Louisiana Space Consortium Graduate Student Research Assistantship and Research Enhancement Award (Grant #NNX15AH82H). Thanks to and the American Association of Petroleum Geologists for supporting my travel to present this work. In addition, thanks to Nicki Button, Glendon Rewerts, and Ashley Hood for their contribution to this project and to this poster presentation.

[1] M. P. Golombek, et. al., "Size-frequency distributions of rocks on the northern plains of Mars with special reference to Phoenix landing surfaces," JGR, Jul. 2008. **[2]** M. P. Golombek, et. al, "Detection and Characterization of Rocks and Rock Size-Frequency Distributions at the Final Four Mars Science Laboratory Landing Sites," Int. J. Mars Sci. Explor., 2012. **[3]** T. de Haas, et. al, "Local late Amazonian boulder breakdown and denudation rate on Mars," GRL, 2013. **[4]** T. C. Orloff, et. al, "Boulder movement at high northern latitudes of Mars," JGR, Nov. 2011. **[5]** P. T. Boggs, et. al, "User's Reference Guide for ODRPACK Version 2 . 01 Software for Weighted Orthogonal Distance Regression," U.S. Dep. Commer., June, p. 99, 1992. **[6]** R. Barnes, et. al, "Priority-flood: An optimal depression-filling and watershed-labeling algorithm for digital elevation models," Comput. Geosci., 2014. **[7]** M. P. Golombek and N. T. Bridges, "Erosion rates on Mars and implications for climate change Constraints from the Pathfinder landing site," 2000. **[8]** N. Krishna and P. S. Kumar, "Impact spallation processes on the Moon: A case study from the size and shape analysis of ejecta boulders and secondary craters of Censorinus crater," Icarus, 2016. **[9]** H. J. Moore and J. M. Keller, "Surface-material maps of Viking landing sites on Mars," A Bibliogr. Planet. Geol. Geophys. Princ. Investig. their Assoc. 1990-1991, 1991.